Ab initio lattice dynamics and structural stability of MgO

Artem R. Oganov[a)]
Department of Earth Sciences, University College London, Gower Street, London WC1E 6BT, United Kingdom

Michael J. Gillan
Department of Physics and Astronomy, University College London, Gower Street, London WC1E 6BT, United Kingdom

G. David Price
Department of Earth Sciences, University College London, Gower Street, London WC1E 6BT, United Kingdom

(Received 22 January 2003; accepted 6 March 2003)

Using density-functional perturbation theory, we have studied lattice dynamics, dielectric and thermodynamic properties, and $P-T$ stability fields of the NaCl- (''B1'') and CsCl- (''B2'') structured phases of MgO. The results compare well with available experiments and resolve the controversy between earlier theoretical studies of the phase diagram of MgO. We predict that at all conditions of the Earth's mantle the B1 structure is stable. Static calculations predict the B1–B2 transition to occur at 490 GPa; zero-point vibrations lower this pressure by 16 GPa. The B2-structured phase is dynamically unstable below 110 GPa, but becomes dynamically stable at higher pressures. On the contrary, the B1 phase does not display soft modes at any of the studied pressures. MgO remains an insulator up to ultrahigh pressures: we predict metallization of the B2-structured phase of MgO at 20.7 TPa. © *2003 American Institute of Physics.*
[DOI: 10.1063/1.1570394]

I. INTRODUCTION

MgO is a material of key importance to Earth sciences and solid-state physics: it is one of the most abundant minerals in the Earth (especially its lower mantle) and a prototype material for a large group of ionic oxides. Remarkably, MgO is among the least polymorphic solids known—only one solid phase, with the NaCl (B1) structure type has been observed in experiments spanning pressures up to 227 GPa[1] and temperatures up to several thousand degrees Kelvin. Early theoretical calculations[2] found that an anti-NiAs-type structure might become marginally stable at high pressures (~200 GPa) before the transition to the CsCl-type (B2) structure, but later[3] both NiAs and anti-NiAs structures were ruled out and it was proposed that the NaCl-structured phase of MgO transforms directly into the CsCl-structured one. In fact, for highly ionic compounds both the NiAs and anti-NiAs structures are destabilized by close cation–cation (for NiAs structure type) or anion–anion (for anti-NiAs type) contacts, and their appearance would be a sign of reduced ionicity of bonding (as probably is the case for BaO, where the NiAs-type structure has been observed at high pressure—Ref. 4) or even metallization. Although at sufficiently high compression all materials should become metallic, MgO is expected to be very difficult to metallize. Our calculations (see the following) show that metallization of MgO occurs at extremely high pressures (20.7 TPa).

The predicted B1–B2 transition pressure is high—its best estimate is 510 GPa.[3,5–7] This exceeds the pressure in the center of the Earth by 40%! This extraordinary structural stability makes MgO suitable as a pressure standard in high-pressure experiments. First attempts to create an MgO-based pressure scale have been undertaken using experiments[8] and molecular dynamics simulations[9] based on an accurate representation of interatomic interactions.

It should be noted that the B1–B2 transition has not yet been reached in experiments and, from theory, only the B1–B2 transition pressure at 0 K is relatively well known (but without account for zero-point vibrations). Two independent recent studies[10,11] addressed the effect of temperature on the B1–B2 transition, but arrived at rather different conclusions. Thermal effects were found to be rather modest by Strachan *et al.*,[10] whereas Drummond and Ackland[11] found a dramatic lowering of the transition pressure with temperature, at the rate of 50 GPa per 1000 K.

The method used in Ref. 10 was based on an interatomic potential model fitted to their static *ab initio* pseudopotential calculations (atomic charges were found independently to be $+0.7$ and -0.7, unusually low values for MgO), whereas *ab initio* frozen-phonon calculations of Ref. 11 suffered from a very approximate account of long-range forces in constructing the dynamical matrix and calculating phonon frequencies. Greater precision and accurate account of the long-range forces may be achieved by using density-functional perturbation theory,[12–15] which is employed in our calculations. Such calculations do not only give more accurate results, but can shed light on the possible deficiencies of the more approximate methods used before. Strachan *et al.*[10,16]

a)Author to whom all correspondence should be addressed. Present address: Laboratory of Crystallography, Department of Materials, ETH Zurich, CH-8092 Zurich, Switzerland. Electronic mail: a.oganov@mat.ethz.ch

TABLE I. Calculated and measured physical properties of MgO (B1 structure). [Lattice parameter and unit cell volume are for the cubic cell. Equation of state in all cases was fitted to the third- or fourth-order Birch–Murnaghan forms (K_0'' given in parentheses indicates the value from the third-order Birch–Murnaghan equation). All theoretical results, except b, are for the athermally optimized structures. b and experimental values are at $P=0$ and $T=300$ K.]

Properties	LDA[a]	LDA[b]	LDA[c]	LDA[d]	GGA[e]	Experiment
a_0 (Å)	4.240	4.222	4.25	4.167	4.253	4.212
V_0 (Å^3)	76.2	75.2	76.8	72.4	77.0	74.7[f]
K_0 (GPa)	172.6	159	159.7	172	150.6	160.2[f]
K_0'	4.004	4.30	4.26	4.09	4.103	3.99[f]
K_0'' (GPa^{-1})	−0.025	−0.030	−0.026	(−0.023)	(−0.027)	(−0.024)[f]
P_{tr} (B1–B2) (GPa)	490	⋯	451	510	509	>227
ϵ_∞	3.15	3.10	⋯	⋯	⋯	2.95
ϵ_0	8.87	⋯	⋯	⋯	⋯	9.64[g]
C_V (300 K) (J mol^{-1} K^{-1})	36.58[h]	36.54[h]	⋯	⋯	⋯	36.87[h]
S (300 K) (J mol^{-1} K^{-1})	26.81	26.65	⋯	⋯	⋯	27.13[h]

[a]This work. LDA+pseudopotentials.
[b]Reference 40. LDA+pseudopotentials.
[c]Reference 41. LDA+pseudopotentials.
[d]Reference 3. All-electron (LAPW) LDA calculations.
[e]Reference 5. All-electron (PAW) GGA calculations.
[f]Experimental data of Ref. 42.
[g]Data of Ref. 43 at 300 K. At 0 K $\epsilon_0=9.34$.
[h]Experimental data of Ref. 44. For calculations of Ref. 40 and experimental data C_V was recalculated from the published C_P using $C_P=C_V(1+\alpha\gamma T)$ and published thermal expansion and Grüneisen parameters.

have also calculated the melting curve of MgO, which is a subject of great geophysical importance and a major controversy between theoretical calculations[17–20] and experiment.[21] The quasiharmonic approximation, employed here, cannot be used to study melting, but can be used to verify the validity of the interatomic potential used by Strachan *et al.* (Ref. 10, see also Ref. 16) by checking the accuracy of their calculated solid–solid (B1–B2) equilibrium line on the phase diagram.

In the following we present results on the $P-T$ equilibrium line separating the stability fields of the MgO polymorphs, as well as a number of properties of these phases (equations of state, thermodynamic, dielectric properties, phonon dispersion curves and phonon densities of states, thermodynamic functions) at both ambient and high pressures. Our results are in excellent agreement with available experimental and theoretical studies and broadly support the phase diagram of MgO calculated by Strachan *et al.* (Ref. 10).

II. COMPUTATIONAL METHODOLOGY

The present results have been obtained with the use of the ABINIT code,[22] a common project of the Université Catholique de Louvain, Corning Incorporated, and other contributors [URL http://www.abinit.org], based on pseudopotentials and plane waves. It relies on an efficient fast Fourier transform algorithm[23] for the conversion of wave functions between real and reciprocal space, on the adaptation to a fixed potential of the band-by-band conjugate gradient method,[24] and on a potential-based conjugate-gradient algorithm for the determination of the self-consistent potential.[25] Technical details on the computation of responses to atomic displacements and homogeneous electric fields can be found in Ref. 14, and the subsequent computation of dynamical matrices, Born effective charges, dielectric permittivity tensors, and interatomic force constants was described in Ref. 15. The calculations were performed using a parallel version of ABINIT on an SGI Origin 3000 parallel computer of CSAR at Manchester University Computer Center.

The local density approximation (LDA)[26] was used for the exchange-correlation. The pseudopotentials used are of the Troullier–Martins[27] type, fully nonlocal and including partial core corrections;[28] the core radii are 0.766 Å for O($1s^2$ core) and 1.371 Å for Mg($1s^22s^22p^6$ core). Table I shows some results of these calculations in comparison with other calculations and experiment. Good agreement with experiment and with all-electron calculations gives evidence of accuracy of the LDA and the pseudopotentials used.

The exchange-correlation functional is the only approximate ingredient in density functional theory.[29,30] Currently the most advanced approximation, the GGA (generalized gradient approximation: see Ref. 31 for reviews of approximate functionals) is applicable to a wider range of problems than the LDA and is better suited for calculations of cohesion energies, studies of atoms, molecules, surfaces, reaction dynamics, and weakly bound systems. It is also known that the LDA often underestimates phase transition pressures, whereas the GGA often gives predictions very close to or slightly higher than experimental transition pressures.[32,33] For the transition from the NaCl-type to the CsCl-type structure in MgO, however, the GGA and LDA give exactly the same pressures, about 510 GPa.[3,5–7] In this study, we decided to use the LDA instead of the GGA, which we used in our recent works,[5,33–37] in view of the equal performance of these approximations for the purposes of this work.

For the B1 phase we have performed calculations at 0, 400, 600 GPa, and at 12 lattice parameters: 8.2, 8.0,...,6.0 bohr[38] (parameters of the cubic face-centered cell are given, although in calculations we actually used the primitive rhombohedral cell containing two atoms) corresponding to the

pressure range from −10 to 780 GPa. Calculations on the B2 phase were done at 0, 400, 600 GPa, and 14 lattice parameters: 5.2, 5.0, 4.8, 4.6, 4.5, 4.4,...,3.6 bohr corresponding to pressures between −16 and 1100 GPa.

The Brillouin zone was sampled with 8×8×8 Monkhorst–Pack[39] meshes; this gave results converged to 0.01 GPa for pressure, 4×10^{-3} eV for the total energy, and 3×10^{-4} eV for the energy differences between the polymorphs. The plane wave kinetic energy cutoff of 40 Ha[38] gave pressure converged to 0.04 GPa, total energy to 0.02 eV, and energy differences to 4×10^{-4} eV. The ground state was found self-consistently (typical convergence 10^{-11} eV). These settings enabled convergence of the phonon frequencies to within 2–5 cm^{-1}.

Response function calculations were performed on a 4×4×4 grid of **q** points in the Brillouin zone, including the Γ point, and provided not only the dynamical matrices and phonon frequencies, but also responses to the electric fields, Born dynamical charges, and high-frequency dielectric constant (ϵ_∞). The dynamical matrices calculated on the 4×4×4 grid of **q** points were split into the short-range and long-range parts; the short-range parts were Fourier transformed, yielding the short-range interatomic force constants corresponding to a 4×4×4 real-space supercell (128 atoms). We checked that errors due to the finite size of this supercell are typically within 2 cm^{-1} (for very few frequencies up to 14 cm^{-1}). From these force constants plus long-range electrostatic terms (described by Born charges and dielectric constants ϵ_∞), dynamical matrices were constructed and diagonalized on a dense grid of **q** points (typically 80×80×80 or denser), yielding a large (several million) number of phonon frequencies at each volume, which were used to calculate the phonon density of states $g(\omega)$ and thermodynamic properties, e.g., heat capacity C_V, entropy S, and Helmholtz free energy F, as a function of temperature:

$$C_V(T)=k_B\int_0^{\omega_{\max}}\left(\frac{\hbar\omega}{k_BT}\right)^2\frac{\exp\left(\frac{\hbar\omega}{k_BT}\right)}{\left(\exp\left(\frac{\hbar\omega}{k_BT}\right)-1\right)^2}g(\omega)d\omega, \tag{1}$$

$$S(T)=\int_0^{\omega_{\max}}\left\{-k_B\ln\left[1-\exp\left(-\frac{\hbar\omega}{k_BT}\right)\right]+\frac{1}{T}\frac{\hbar\omega}{\exp\left(\frac{\hbar\omega}{k_BT}\right)-1}\right\}g(\omega)d\omega, \tag{2}$$

$$F(T)=E_0+\int_0^{\omega_{\max}}\left\{\frac{\hbar\omega}{2}+k_BT\times\ln\left[1-\exp\left(-\frac{\hbar\omega}{k_BT}\right)\right]\right\}g(\omega)d\omega, \tag{3}$$

where E_0 is the energy of the static lattice. Using the same force constants, dynamical charges, and high-frequency dielectric constants, we calculated phonon dispersion curves and static dielectric constants (ϵ_0).

III. RESULTS

A. Lattice dynamics of the B1 phase

Phonon dispersion curves of MgO have been experimentally studied in Refs. 45 and 46; infrared spectra were studied in Ref. 43. Pioneering calculations of Schütt *et al.*[47] have demonstrated the great capabilities of density-functional perturbation theory for studies of lattice dynamics. Subsequently, lattice dynamics of MgO was studied in Ref. 40 with the same method and in Refs. 48 and 11 using the frozen-phonon technique with corrections for long-range forces. Density-functional perturbation theory is the better method, because it naturally and properly takes into account long-range electrostatic forces and can describe, for example, LO–TO splitting in ionic solids and requires no *ad hoc* assumptions about the values of the dynamical charges and dielectric constants.

Figure 1(a) shows that good agreement exists between the theoretical and experimental phonon dispersion curves. As is clear from Table I, our lattice-dynamical calculations give thermodynamic properties in excellent agreement with experiment. Figure 1 also shows theoretical phonon dispersion curves and phonon densities of states at 400 and 600 GPa (400 GPa is still within the stability field of the B1 structure, while 600 GPa is in the stability field of the B2 structure). At all these pressures, the structure remains dynamically stable, the phonon spectrum extends to higher frequencies, acquires a more complicated structure, and a pseudogap develops in the middle of the spectrum.

B. Lattice dynamics of the B2 phase

To our knowledge, the only previous study of the lattice dynamics of this phase is that done by Drummond and Ackland.[11] Figure 2 shows our phonon dispersion curves of the CsCl-structured phase of MgO at 0, 400, and 600 GPa, and phonon densities of states at 400 and 600 GPa. This phase is dynamically unstable and has whole soft phonon branches at 0 GPa, as can be seen in Fig. 2(a). However, it becomes dynamically stable above 110 GPa (above 82 GPa according to Ref. 11). Dynamical instability means that this phase, thermodynamically stable at very high pressures (see the following), cannot be decompressed below 110 GPa.

C. Dielectric constants and Born effective charges

The calculated Born dynamical charges and dielectric constants of the B1 and B2 phases are shown in Fig. 3 as a function of pressure. For the B2 phase we show these properties only in the region of its dynamical stability.

In both phases the dynamical charges are close to the formal ionic values of +2 for Mg and −2 for O and slowly decrease with pressure. This confirms the expected high degree of ionicity for MgO (which is higher in the B2 structure) and its decrease with pressure, although one should remember that dynamical charges are not a rigorous measure of ionicity—see, e.g., Ref. 49.

As is clear from Table I, theory is able to predict dielectric properties within an ~10% uncertainty, and it is well

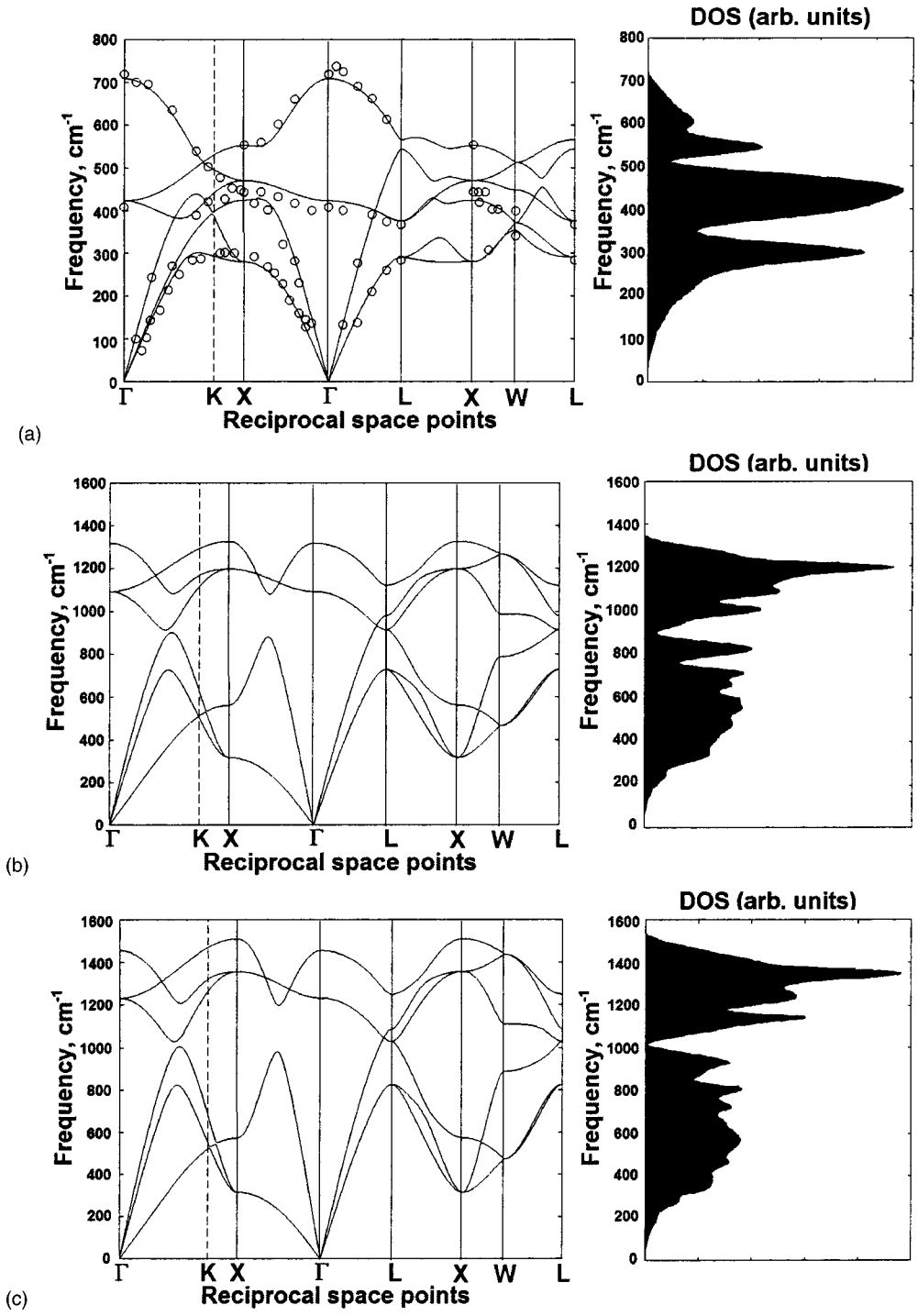

FIG. 1. Phonon dispersion curves and phonon spectra of MgO in the NaCl structure. (a) At 0 GPa, (b) at 400 GPa, (c) at 600 GPa. Experimental data at 0 GPa (Refs. 43, 45, and 46) are shown in (a) by open circles. Special points of the Brillouin zone: $\Gamma=[000]$, $X=[\frac{1}{2};\frac{1}{2};0]$, $K=[\frac{3}{8};\frac{3}{8};\frac{3}{4}]$, $L=[\frac{1}{2};\frac{1}{2};\frac{1}{2}]$, $W=[\frac{1}{2};\frac{1}{4};\frac{3}{4}]$. Expressed in the cubic setting, these points are: $\Gamma=[000]$, $X=[\frac{1}{2};0;0]$, $K=[\frac{3}{8};\frac{3}{8};0]$, $L=[\frac{1}{4};\frac{1}{4};\frac{1}{4}]$, $W=[\frac{1}{4};\frac{1}{2};0]$.

known that the LDA overestimates the high-frequency dielectric constants (see Ref. 50 for a discussion). As shown in Fig. 3(b), the high-frequency dielectric constants of both phases do not change significantly with pressure; their initial small decrease with pressure is followed by a tiny increase above 320 GPa for the B1 phase and above ~900 GPa for the B2 phase. This can be rationalized by expressing the high-frequency dielectric constant via the ionic polarizabilities using the Clausius–Mossotti equation:

$$\frac{\epsilon_\infty-1}{\epsilon_\infty+2}=\sum_i \frac{4\pi}{3}\frac{n_i\alpha_i}{V_m}, \tag{4}$$

equivalently recast as

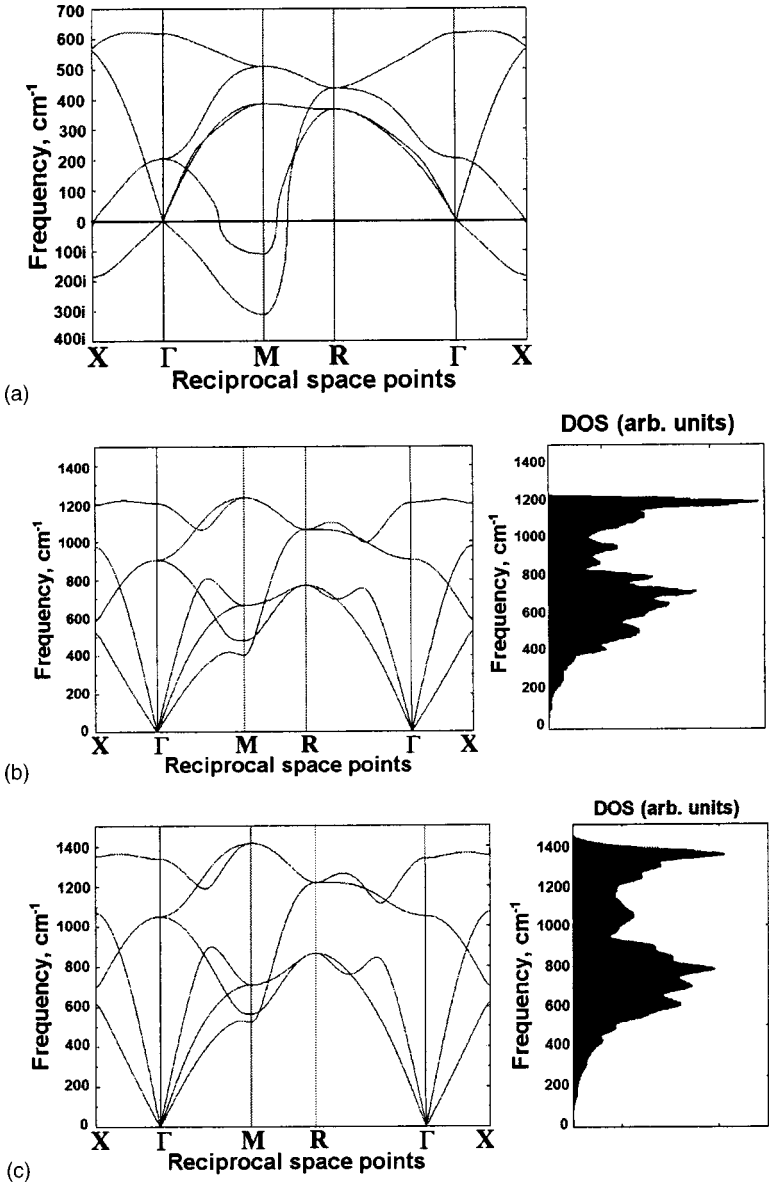

FIG. 2. Phonon dispersion curves and phonon spectra of MgO in the CsCl structure. (a) At 0 GPa, (b) at 400 GPa, (c) at 600 GPa. Special points of the Brillouin zone: $\Gamma=[000]$, $X=[\frac{1}{2};0;0]$, $M=[\frac{1}{2},\frac{1}{2};0]$, $R=[\frac{1}{2};\frac{1}{2};\frac{1}{2}]$. Whole phonon branches with imaginary frequencies can be seen in (a), indicating the dynamical instability of this structure at low pressures.

$$\epsilon_\infty = \frac{2\Sigma_i \frac{4\pi}{3}\frac{n_i\alpha_i}{V_m}+1}{1-\Sigma_i \frac{4\pi}{3}\frac{n_i\alpha_i}{V_m}}, \tag{5}$$

where α_i is the polarizability and n_i the number (per molar volume V_m of the crystal) of ith type ions. The ionic polarizability is proportional to the ionic volume, and hence the ratio $n_i\alpha_i/V_m$ and ϵ_∞ for wide-gap insulators with closed-shell ions should be nearly independent of pressure [and almost independent of structure, as can be seen in Fig. 3(b)]. The predicted small dependence on pressure can be understood by noting that the dielectric constant of MgO is dominated by the electronic polarizability of the O^{2-} anions.[51] Since the O^{2-} ions are more compressible than Mg^{2+} ions and the volume and polarizability of O^{2-} are expected to decrease with pressure faster than V_m (i.e., the ratio $n_i\alpha_i/V_m$ for O^{2-} should decrease), ϵ_∞ too can be expected to decrease until the contribution from Mg^{2+} becomes comparable with that of O^{2-}.

The static dielectric constant can be represented as a sum of the high-frequency constant (due to electronic polarizability) and the ionic-displacement polarizability contribution. Given the nearly constant values of ϵ_∞, the rapid decrease of the static dielectric constants with pressure [Fig. 3(a)] is mainly due to the decrease of the displacement polarizability related to the increase of the phonon frequencies with pressure.

D. B1–B2 phase transition

Figure 4(a) shows the calculated static enthalpies of the B1 and B2 structures and their crossover, corresponding to a first-order phase transition at 490 GPa, close to the most accurate currently available estimate from all-electron calculations, 510 ± 5 GPa.[3,5–7] Table II gives equation of state parameters of both phases obtained by fitting of the calculated $E(V)$ data to the Vinet (Refs. 52 and 53, see also Ref. 54) function:

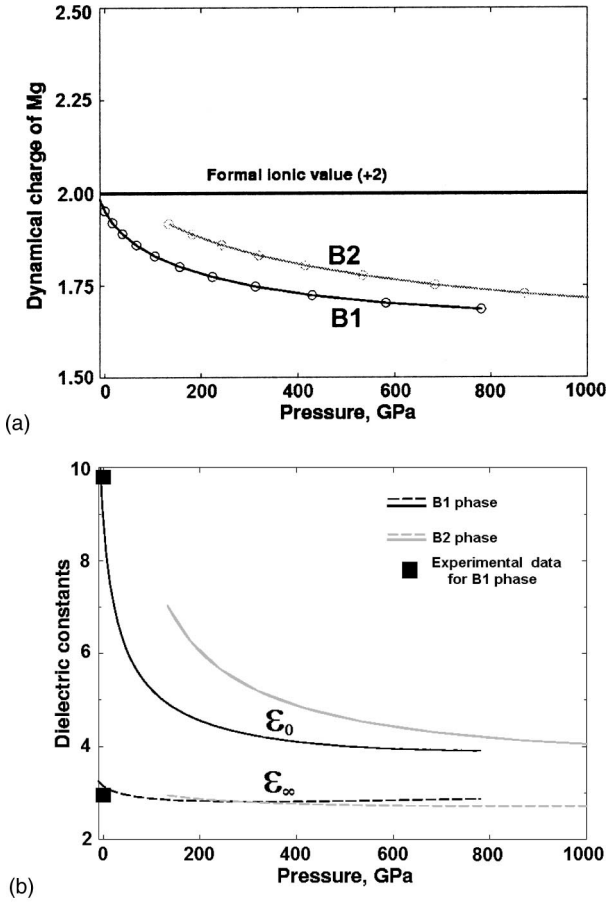

FIG. 3. (a) Born dynamical charge of Mg and (b) dielectric constants as a function of pressure. Dynamical charge of O is equal to minus the Mg charge and not shown here.

$$E(V)=E(V_0)+\frac{9K_0V_0}{\eta^2}\{1-[1-\eta(1-x)]\exp[\eta(1-x)]\}, \tag{6}$$

where $x=(V/V_0)^{1/3}$, $\eta=\frac{3}{2}(K_0-1)$. The corresponding $P(V)$ equation of state is

$$P(V)=-3K_0x^{-2}(1-x)\exp[\eta(1-x)]. \tag{7}$$

At the transition pressure, we find the difference of volumes $\Delta V_{\mathrm{B1-B2}}(P_{\mathrm{tr}})=0.298\,\text{Å}^3$, static energies $\Delta E_{\mathrm{B1-B2}}(P_{\mathrm{tr}})=0.91\,\mathrm{eV}$, and zero-point energies

TABLE II. Equation of state parameters of MgO polymorphs. [Values given are per two atoms. The fits were performed in the whole pressure range, from −10 to 780 GPa for the B1 phase, from −16 to 1100 GPa for the B2 phase. It is interesting to note that the present LDA results are much better fitted by the Vinet than by the third-order Birch–Murnaghan equation of state, whereas the opposite is true for our previous all-electron and pseudopotentials GGA results (Ref. 5).]

Structure	$E(V_0)$ (eV)	V_0 (Å^3)	K_0 (GPa)	K_0'
B1	−485.09	19.04	168.92	4.28
B2	−483.69	18.32	160.20	4.51

$\Delta E^{\mathrm{ZP}}_{\mathrm{B1-B2}}(P_{\mathrm{tr}})=0.023\,\mathrm{eV}$ (per two atoms). To the first level of approximation the shift of the transition pressure due to zero-point vibrations is

$$\Delta P^{\mathrm{ZP}}\approx-\frac{\Delta E^{\mathrm{ZP}}(P_{\mathrm{tr}})}{\Delta V(P_{\mathrm{tr}})}=-12.3\,\mathrm{GPa}.$$

More accurate calculations give −16 GPa (see the following).

We calculate the Gibbs free energy G from the Helmholtz free energy as $G(P,T)=F(V,T)+PV$, where $P=-(\partial F/\partial V)_T$ and at each temperature $F(V,T)$ was fitted by the Vinet function (6), giving an analytical thermal equation of state, and all thermodynamic functions interpolated as a function of volume. Figures 4(b) and 4(c) show the calculated Gibbs free energies as a function of pressure at 100 K (transition pressure 474 GPa, which is 16 GPa lower than the static result, almost entirely due to zero-point vibrations) and 3000 K (transition pressure 443 GPa), respectively. We have calculated the whole $P-T$ phase equilibrium line by this method (closed circles in Fig. 5), but since the analytical fits of $F(V)$ have small errors, the results have an uncertainty of several GPa and Clapeyron slopes dP/dT are not very precise.

However, the Clapeyron slope can be determined with great precision from the Clausius–Clapeyron relation ($dP/dT=\Delta S/\Delta V$); at 3000 K and 443 GPa it is equal to 16×10^{-3} GPa/K and changes by less than 3% when pressure changes by 10 GPa. Proceeding iteratively from 3000 K to lower and higher temperatures by calculating the slope at each P/T point, we have obtained a number of Clapeyron slopes at different points of the phase diagram. In this way we also found the transition pressure of 473.5 GPa at 100 K,

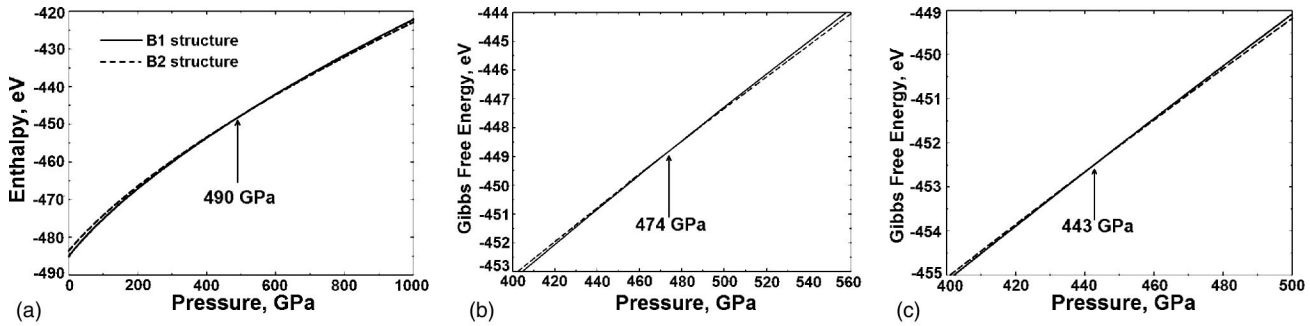

FIG. 4. B1–B2 transition in MgO: static results (a), results at 100 K (b), and 3000 K (c).

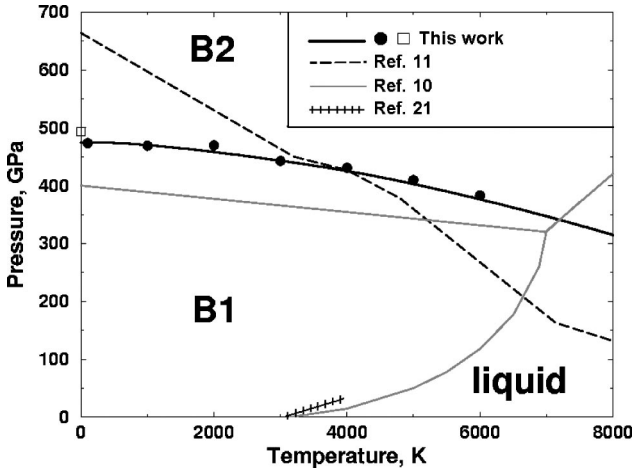

FIG. 5. Phase diagram of MgO. Calculations of this work: solid black line—result of integration of the Clapeyron slopes, closed circles—direct calculations, open square—static transition pressure. Also shown are theoretical results of Refs. 10 and 11 and experimental melting curve of Ref. 21.

consistent with Fig. 4 and with our estimates of the effect of the zero-point vibrations on the transition pressure. The phase equilibrium line, shown in Fig. 5, was obtained by integrating the spline-interpolated dP/dT slopes at 100, 500, 1000,...,2500, 3000, 4000,...,6000 K: $P(T)=P(0\ \mathrm{K})+\int_0^T (dP/dT)dT$ and taking the transition pressure at 0 K equal to 474 GPa (including the effect of zero-point vibrations). Beyond 6000 K the equilibrium line was extrapolated. This equilibrium line is smooth, has reliable Clapeyron slopes, and agrees very well with the direct calculations based on the Gibbs free energy.

We see that the calculated phase equilibrium line is much more similar to the results of Strachan *et al.*[10] than to those of Drummond and Ackland.[11] The main difference between present results and those of Ref. 10 is that their transition pressures are ~90 GPa lower than ours and 110 GPa lower than from all-electron calculations (this is probably due to the pseudopotentials they used), whereas the slopes are very similar to ours. Drummond and Ackland[11] have obtained a much higher transition pressure at 0 K (664 GPa), apparently due to the pseudopotential error; their dP/dT slopes are also significantly different, probably as a result of an approximate treatment of long-range forces in the dynamical matrix and (or) the pseudopotential error.

One can see that at 0 K the slope dP/dT is zero, as it should be (at 0 K entropies of both phases are zero and $\Delta S=0$, which means that $dP/dT=\Delta S/\Delta V=0$). This feature cannot be seen in the results of Ref. 10, because the phase diagram calculated in Ref. 10 was based on the classical approximation, which is not designed to study such essentially quantum effects.[55] Drummond and Ackland[11] did not see this feature in their lattice-dynamical calculations and argued that this could be due to small ΔV, however, we find that the volume change is not very small: our all-electron GGA calculations[5] resulted in $\Delta V/V=4.8\%$, and pseudopotential LDA calculations presented here give $\Delta V/V=3.25\%$.

As our results overall support the results of Strachan *et al.*[10] for the solid phases, it can be speculated that the interatomic potential model they used is likely to produce results close to full *ab initio* calculations of the melting curves for the B1 and B2 phases. Following criticism of their methodology,[56] Strachan *et al.*[16] were able to show that their melting curve is reproduced by two-phase molecular dynamics simulations using the same interatomic potential and therefore ultimately hinges only on the validity of that potential model. The melting curve of Strachan *et al.*[10] for the B1-structured phase is in good agreement with available atomistic[18–20] and semiempirical[17] molecular dynamics simulations. However, all these theoretical calculations are in sharp conflict with experimental results,[21] which give much lower high-pressure melting temperatures.

E. Metallization at ultrahigh pressures

According to our calculations, MgO remains nonmetallic throughout the pressure range studied here (0–1000 GPa) in both the B1 and B2 structures. It can be expected that metallization of MgO would require extremely high pressures: MgO is a wide-gap insulator with low compressibility and is isoelectronic with Ne, which is believed to be the hardest solid to metallize (with metallization pressure estimated as 158 TPa[57] and 134 TPa[58]).

We have explored the metallization of the B2 structure using two sets of calculations with very dense **k**-point sampling (24×24×24) and Gaussian smearing technique (with the electronic "temperature" of 0.2 eV) appropriate for the metallic state. One set of calculations employed the LDA, the same pseudopotentials as used throughout this paper, and much higher plane-wave cutoff of 100 Ha. In these calculations, metallization was found to occur at the unit cell volume of 1.95 Å^3 (ninefold compression, pressure 13.4±0.2 TPa). At such extreme compressions pseudopotential calculations may give lower pressures compared to all-electron calculations because of the neglect of the core–core overlap. Another set of calculations used the GGA,[59] frozen-core all-electron PAW method[60,61] as implemented in the VASP[62] code, and cutoffs of 100 Ha for plane waves and 200 Ha for the augmentation charges. In these calculations (with $1s^2$ core for O and $1s^2 2s^2$ core for Mg) we found metallization at the pressure of 20.7±0.5 TPa (volume 2.07 Å^3). Our estimates of the metallization pressure (preferred value 20.7 TPa) confirm that MgO is among the hardest solids to metallize.

IV. DISCUSSION

MgO is one of the simplest and most important materials for mineral physics and solid-state physics. It is one of the most abundant minerals in the Earth, a prototypic ionic oxide serving as a classical illustration of the importance of many-body interactions, and one of the most studied materials by both theoretical and experimental methods. In our previous work,[5] using *ab initio* static and molecular dynamics simulations, we have studied its equation of state, elasticity, anharmonicity, and structural stability at 0 K.

In this work, using density-functional perturbation theory, we have studied lattice dynamics, dielectric properties, and phase transition of MgO from the NaCl ("B1") to

the CsCl (''B2'') structure. This is one of the first applications of density-functional perturbation theory to the prediction of $P-T$ phase diagrams of materials (see also Refs. 63 and 64). This method, having a sound theoretical grounding and combining high numerical precision with a direct approach to thermodynamic properties of solids, surely has a great potential for such applications. The only approximations made in this work were—(1) LDA for the exchange-correlation energy, (2) pseudopotential description of the core–valence interaction, (3) quasiharmonic approximation. Comparison with all-electron calculations and experiment shows that the first two approximations (for the properties calculated here) are moderate. The quasiharmonic approximation is known to break down at temperatures above 50%–70% of the melting temperature. Earlier,[5] using *ab initio* molecular dynamics simulations, we have shown that intrinsic anharmonic effects (which are neglected in the quasiharmonic approximation) make a major contribution to the thermal expansion at 1 atm and $T>2000$ K, but become very small at 50 GPa and above. At pressures of 400–600 GPa, one would expect that the quasiharmonic approximation remains valid for MgO up to 4000–5000 K. We have demonstrated good agreement between theory and available experiments and calculated a number of properties (phonon dispersion curves and densities of states, Born charges, dielectric constants) at both ambient and ultrahigh pressures. In good agreement with the best all-electron *ab initio* calculations, we find the static pressure of the B1–B2 transition to be 490 GPa; due to the zero-point vibrations, the transition pressure at 0 K is 16 GPa lower (474 GPa).

The CsCl-structured phase is found to be dynamically unstable below 110 GPa, therefore, it will not be possible to decompress it below that pressure. Our calculated $P-T$-equilibrium line for the B1–B2 transition broadly supports previous results of Strachan *et al.*[10] MgO is predicted to have the NaCl structure at all $P-T$ conditions within the Earth and well beyond. It would be interesting to use *ab initio* methods (*ab initio* molecular dynamics is the most suitable method for this) for the calculation of the melting curve of MgO, as there is a sharp conflict between the existing experiments[21] and atomistic[18–20] and semiempirical[17] theoretical results. Resolving this controversy would reveal the problems with existing theoretical or experimental methods and will be an important step toward understanding the partial melting of the Earth's lower mantle at the boundary with the core[19,65] and core-mantle equilibration processes.

It is interesting to note the early hypothesis by Ramsey (for a discussion see Ref. 66) that the Earth's core consists of the same materials as the Earth's mantle (e.g., MgO and silicates of Mg), but which have undergone major densification and (to explain the Earth's magnetic field) metallization under pressure. Now, of course, it is well established that the Earth's core is made of iron-rich alloys. It is also well established (see Ref. 67) that silicates of the Earth's mantle do not undergo metallization at the pressure of the core-mantle boundary (136 GPa). Here we find that in both the B1 and B2 structures MgO remains nonmetallic up to ultrahigh pressures; using all-electron calculations we have predicted that the high-pressure B2 phase becomes a metal only at the pressure of 20.7 TPa, thus putting MgO in the list of the most difficult solids to metallize. This is not very surprising, as MgO is a wide-gap ionic insulator that can be regarded as isoelectronic to Ne, for which the highest metallization pressure (134–158 TPa) has been predicted.[57,58] Bukowinski[68] had argued that in order to seriously disrupt the valence electronic shells of atoms, pressures of the order of one atomic unit of pressure (29.4 TPa) are required. The metallization pressure of MgO that we find is close to this order-of-magnitude estimate. Lower metallization pressure in MgO compared to Ne can be related to weaker binding of the valence electrons in O^{2-} ions compared to the isoelectronic Ne atoms.

ACKNOWLEDGMENTS

One of the authors (A.R.O.) would like to thank NERC (Grant No. GR3/12083) for funding, and Douglas C. Allan, Xavier Gonze, Stewart J. Clark, Dario Alfè, A. Marshall Stoneham, and Anthony H. Harker for discussions. A. Khein and D. C. Allan have provided the pseudopotentials used in this work. We are grateful to the ABINIT group for making their code publicly available, to Georg Kresse for the permission to use his VASP code in this work, and to Jon Gibson of Manchester Computer Center (MCC) for help with compiling a parallel version of ABINIT. NERC has provided access to the SGI Origin 3000 and CRAY T3E parallel computers at MCC via the Computational Mineral Physics Consortium.

[1] T. S. Duffy, R. J. Hemley, and H.-K. Mao, Phys. Rev. Lett. **74**, 1371 (1995).
[2] M. Causà, R. Dovesi, C. Pisani, and C. Roetti, Phys. Rev. B **33**, 1308 (1986).
[3] M. J. Mehl, R. E. Cohen, and H. Krakauer, J. Geophys. Res. [Solid Earth] **93**, 8009 (1988).
[4] S. T. Wier, Y. K. Vohra, and A. L. Ruoff, Phys. Rev. B **33**, 4221 (1986).
[5] A. R. Oganov and P. I. Dorogokupets, Phys. Rev. B (to be published).
[6] J. E. Jaffe, J. A. Snyder, Z. Lin, and A. C. Hess, Phys. Rev. B **62**, 1660 (2000).
[7] M.-P. Habas, R. Dovesi, and A. Lichanot, J. Phys.: Condens. Matter **10**, 6897 (1998).
[8] C.-S. Zha, H.-K. Mao, and R. J. Hemley, Proc. Natl. Acad. Sci. U.S.A. **97**, 13494 (2000).
[9] M. Matsui, S. C. Parker, and M. Leslie, Am. Mineral. **85**, 312 (2000).
[10] A. Strachan, T. Çağin, and W. A. Goddard III, Phys. Rev. B **60**, 15084 (1999).
[11] N. D. Drummond and G. J. Ackland, Phys. Rev. B **65**, 184104 (2002).
[12] S. Baroni, P. Gianozzi, and A. Testa, Phys. Rev. Lett. **58**, 1861 (1987).
[13] S. Baroni, S. de Gironcoli, A. Dal Corso, and P. Gianozzi, Rev. Mod. Phys. **73**, 515 (2001).
[14] X. Gonze, Phys. Rev. B **55**, 10337 (1997).
[15] X. Gonze and C. Lee, Phys. Rev. B **55**, 10355 (1997).
[16] A. Strachan, T. Çağin, and W. A. Goddard III, Phys. Rev. B **63**, 096102 (2001).
[17] R. E. Cohen and Z. Gong, Phys. Rev. B **50**, 12301 (1994).
[18] A. B. Belonoshko and L. S. Dubrovinsky, Am. Mineral. **81**, 303 (1996).
[19] A. B. Belonoshko and L. S. Dubrovinsky, Geochim. Cosmochim. Acta **60**, 1645 (1996).
[20] L. Vočadlo and G. D. Price, Phys. Chem. Miner. **23**, 42 (1996).
[21] A. Zerr and R. Boehler, Nature (London) **371**, 506 (1994).
[22] X. Gonze, J.-M. Beuken, R. Caracas *et al.*, Comput. Mater. Sci. **25**, 478 (2002).
[23] S. Goedecker, SIAM J. Sci. Comput. (USA) **18**, 1605 (1997).
[24] M. C. Payne, M. P. Teter, D. C. Allan, T. A. Arias, and J. D. Joannopoulos, Rev. Mod. Phys. **64**, 1045 (1992).
[25] X. Gonze, Phys. Rev. B **54**, 4383 (1996).

[26] J. P. Perdew and Y. Wang, Phys. Rev. B **45**, 13244 (1992).
[27] N. Troullier and J. L. Martins, Phys. Rev. B **43**, 1993 (1991).
[28] S. G. Louie, S. Froyen, and M. L. Cohen, Phys. Rev. B **26**, 1738 (1982).
[29] P. Hohenberg and W. Kohn, Phys. Rev. **136**, B864 (1964).
[30] W. Kohn and L. J. Sham, Phys. Rev. **140**, A1133 (1965).
[31] J. P. Perdew and S. Kurth, in *Density Functionals: Theory and Applications*, edited by D. P. Joubert Lect. Notes Phys. **500** (Springer, Berlin, 1998), pp. 8–59; S. Kurth, J. P. Perdew, and P. Blaha, Int. J. Quantum Chem. **75**, 889 (1999).
[32] A. Zupan, P. Blaha, K. Schwarz, and J. P. Perdew, Phys. Rev. B **58**, 11266 (1998).
[33] A. R. Oganov and J. P. Brodholt, Phys. Chem. Miner. **27**, 430 (2000).
[34] A. R. Oganov, J. P. Brodholt, and G. D. Price, Earth Planet. Sci. Lett. **184**, 555 (2001).
[35] A. R. Oganov, J. P. Brodholt, and G. D. Price, Nature (London) **411**, 934 (2001).
[36] A. R. Oganov, G. D. Price, and J. P. Brodholt, Acta Crystallogr., Sect. A: Found. Crystallogr. **57**, 548 (2001).
[37] J. P. Brodholt, A. R. Oganov, and G. D. Price, Philos. Trans. R. Soc. London, Ser. A **360**, 2507 (2002).
[38] 1 bohr=0.529 177 Å; 1 Ha=27.211 396 eV.
[39] H. J. Monkhorst and J. D. Pack, Phys. Rev. B **13**, 5188 (1976).
[40] B. B. Karki, R. M. Wentzcovitch, S. de Gironcoli, and S. Baroni, Phys. Rev. B **61**, 8793 (2000).
[41] B. B. Karki, L. Stixrude, S. J. Clark, M. C. Warren, G. J. Ackland, and J. Crain, Am. Mineral. **82**, 51 (1997).
[42] S. Speziale, C.-S. Zha, T. S. Duffy, R. J. Hemley, and H.-K. Mao, J. Geophys. Res. [Solid Earth] **106**, 515 (2001).
[43] J. R. Jasperse, A. Kahan, J. N. Plendl, and S. S. Mitra, Phys. Rev. **146**, 526 (1966).
[44] R. A. Robie and B. S. Hemingway, U.S. Geological Survey Bulletin No. 2131, Washington, 1995.
[45] G. Peckham, Proc. Phys. Soc. London **90**, 657 (1967).
[46] M. J. L. Sangster, G. Peckham, and D. H. Saunderson, J. Phys. C **3**, 1026 (1970).
[47] O. Schütt, P. Pavone, W. Windl, K. Karch, and D. Strauch, Phys. Rev. B **50**, 3746 (1994).
[48] K. Parlinski, J. Łażiewski, and Y. Kawazoe, J. Phys. Chem. Solids **61**, 87 (2000).
[49] Ph. Ghosez, J.-P. Michenaud, and X. Gonze, Phys. Rev. B **58**, 6224 (1998).
[50] X. Gonze, Ph. Ghosez, and R. W. Godby, Phys. Rev. Lett. **74**, 4035 (1995).
[51] From Pauling's calculated molar ionic refractions [L. Pauling, Proc. R. Soc. London, Ser. A **114**, 181 (1927)], $\alpha(O^{2-})=3.9$ Å^3 and $\alpha(Mg^{2+})=0.1$ Å^3.
[52] P. Vinet, J. Ferrante, J. R. Smith, and J. H. Rose, J. Phys. C **19**, L467 (1986).
[53] P. Vinet, J. H. Rose, J. Ferrante, and J. R. Smith, J. Phys.: Condens. Matter **1**, 1941 (1989).
[54] J. Hama and K. Suito, J. Phys.: Condens. Matter **8**, 67 (1996).
[55] In classical mechanics, ΔS is finite as $T\rightarrow 0$ K and, therefore, dP/dT tends to a nonzero value as $T\rightarrow 0$ K.
[56] A. B. Belonoshko, Phys. Rev. B **63**, 096101 (2001).
[57] J. Hama, Phys. Lett. A **105**, 303 (1984).
[58] J. C. Boettger, Phys. Rev. B **33**, 6788 (1986).
[59] Y. Wang and J. P. Perdew, Phys. Rev. B **44**, 13298 (1991).
[60] P. E. Blöchl, Phys. Rev. B **50**, 17953 (1994).
[61] G. Kresse and D. Joubert, Phys. Rev. B **59**, 1758 (1999).
[62] G. Kresse and J. Furthmüller, Comput. Mater. Sci. **6**, 15 (1996).
[63] P. Pavone, S. Baroni, and S. de Gironcoli, Phys. Rev. B **57**, 10421 (1998).
[64] K. Gaál-Nagy, M. Schmitt, P. Pavone, and D. Strauch, Comput. Mater. Sci. **22**, 49 (2001).
[65] A. Zerr, A. Diegler, and R. Boehler, Science **281**, 243 (1998).
[66] J.-P. Poirier, *Introduction to the Physics of the Earth's Interior* (Cambridge University Press, Cambridge, 2000).
[67] V. N. Zharkov and V. A. Kalinin, *Equations of State of Solids at High Pressures and Temperatures* (Consultants Bureau, New York, 1971).
[68] M. S. T. Bukowinski, Annu. Rev. Earth Planet Sci. **22**, 167 (1994).